Measurement of time-dependent CP asymmetry in $B^0 \to c\bar{c}K^{(*)0}$ decays

B. Aubert,[1] Y. Karyotakis,[1] J. P. Lees,[1] V. Poireau,[1] E. Prencipe,[1] X. Prudent,[1] V. Tisserand,[1] J. Garra Tico,[2] E. Grauges,[2] L. Lopez,[3a,3b] A. Palano,[3a,3b] M. Pappagallo,[3a,3b] G. Eigen,[4] B. Stugu,[4] L. Sun,[4] M. Battaglia,[5] D. N. Brown,[5] L. T. Kerth,[5] Yu. G. Kolomensky,[5] G. Lynch,[5] I. L. Osipenkov,[5] K. Tackmann,[5] T. Tanabe,[5] C. M. Hawkes,[6] N. Soni,[6] A. T. Watson,[6] H. Koch,[7] T. Schroeder,[7] D. J. Asgeirsson,[8] B. G. Fulsom,[8] C. Hearty,[8] T. S. Mattison,[8] J. A. McKenna,[8] M. Barrett,[9] A. Khan,[9] A. Randle-Conde,[9] V. E. Blinov,[10] A. D. Bukin,[10,*] A. R. Buzykaev,[10] V. P. Druzhinin,[10] V. B. Golubev,[10] A. P. Onuchin,[10] S. I. Serednyakov,[10] Yu. I. Skovpen,[10] E. P. Solodov,[10] K. Yu. Todyshev,[10] M. Bondioli,[11] S. Curry,[11] I. Eschrich,[11] D. Kirkby,[11] A. J. Lankford,[11] P. Lund,[11] M. Mandelkern,[11] E. C. Martin,[11] D. P. Stoker,[11] S. Abachi,[12] C. Buchanan,[12] H. Atmacan,[13] J. W. Gary,[13] F. Liu,[13] O. Long,[13] G. M. Vitug,[13] Z. Yasin,[13] L. Zhang,[13] V. Sharma,[14] C. Campagnari,[15] T. M. Hong,[15] D. Kovalskyi,[15] M. A. Mazur,[15] J. D. Richman,[15] T. W. Beck,[16] A. M. Eisner,[16] C. A. Heusch,[16] J. Kroseberg,[16] W. S. Lockman,[16] A. J. Martinez,[16] T. Schalk,[16] B. A. Schumm,[16] A. Seiden,[16] L. O. Winstrom,[16] C. H. Cheng,[17] D. A. Doll,[17] B. Echenard,[17] F. Fang,[17] D. G. Hitlin,[17] I. Narsky,[17] T. Piatenko,[17] F. C. Porter,[17] R. Andreassen,[18] G. Mancinelli,[18] B. T. Meadows,[18] K. Mishra,[18] M. D. Sokoloff,[18] P. C. Bloom,[19] W. T. Ford,[19] A. Gaz,[19] J. F. Hirschauer,[19] M. Nagel,[19] U. Nauenberg,[19] J. G. Smith,[19] S. R. Wagner,[19] R. Ayad,[20,†] A. Soffer,[20,‡] W. H. Toki,[20] R. J. Wilson,[20] E. Feltresi,[21] A. Hauke,[21] H. Jasper,[21] M. Karbach,[21] J. Merkel,[21] A. Petzold,[21] B. Spaan,[21] K. Wacker,[21] M. J. Kobel,[22] R. Nogowski,[22] K. R. Schubert,[22] R. Schwierz,[22] A. Volk,[22] D. Bernard,[23] G. R. Bonneaud,[23] E. Latour,[23] M. Verderi,[23] P. J. Clark,[24] S. Playfer,[24] J. E. Watson,[24] M. Andreotti,[25a,25b] D. Bettoni,[25a] C. Bozzi,[25a] R. Calabrese,[25a,25b] A. Cecchi,[25a,25b] G. Cibinetto,[25a,25b] P. Franchini,[25a,25b] E. Luppi,[25a,25b] M. Negrini,[25a,25b] A. Petrella,[25a,25b] L. Piemontese,[25a] V. Santoro,[25a,25b] R. Baldini-Ferroli,[26] A. Calcaterra,[26] R. de Sangro,[26] G. Finocchiaro,[26] S. Pacetti,[26] P. Patteri,[26] I. M. Peruzzi,[26,§] M. Piccolo,[26] M. Rama,[26] A. Zallo,[26] R. Contri,[27a,27b] E. Guido,[27b] M. Lo Vetere,[27a,27b] M. R. Monge,[27a,27b] S. Passaggio,[27a] C. Patrignani,[27a,27b] E. Robutti,[27a] S. Tosi,[27a,27b] K. S. Chaisanguanthum,[28] M. Morii,[28] A. Adametz,[29] J. Marks,[29] S. Schenk,[29] U. Uwer,[29] F. U. Bernlochner,[30] V. Klose,[30] H. M. Lacker,[30] D. J. Bard,[31] P. D. Dauncey,[31] M. Tibbetts,[31] P. K. Behera,[32] X. Chai,[32] M. J. Charles,[32] U. Mallik,[32] J. Cochran,[33] H. B. Crawley,[33] L. Dong,[33] W. T. Meyer,[33] S. Prell,[33] E. I. Rosenberg,[33] A. E. Rubin,[33] Y. Y. Gao,[34] A. V. Gritsan,[34] Z. J. Guo,[34] N. Arnaud,[35] J. Béquilleux,[35] A. D'Orazio,[35] M. Davier,[35] J. Firmino da Costa,[35] G. Grosdidier,[35] F. Le Diberder,[35] V. Lepeltier,[35] A. M. Lutz,[35] S. Pruvot,[35] P. Roudeau,[35] M. H. Schune,[35] J. Serrano,[35] V. Sordini,[35,‖] A. Stocchi,[35] G. Wormser,[35] D. J. Lange,[36] D. M. Wright,[36] I. Bingham,[37] J. P. Burke,[37] C. A. Chavez,[37] J. R. Fry,[37] E. Gabathuler,[37] R. Gamet,[37] D. E. Hutchcroft,[37] D. J. Payne,[37] C. Touramanis,[37] A. J. Bevan,[38] C. K. Clarke,[38] F. Di Lodovico,[38] R. Sacco,[38] M. Sigamani,[38] G. Cowan,[39] S. Paramesvaran,[39] A. C. Wren,[39] D. N. Brown,[40] C. L. Davis,[40] A. G. Denig,[41] M. Fritsch,[41] W. Gradl,[41] A. Hafner,[41] K. E. Alwyn,[42] D. Bailey,[42] R. J. Barlow,[42] G. Jackson,[42] G. D. Lafferty,[42] T. J. West,[42] J. I. Yi,[42] J. Anderson,[43] C. Chen,[43] A. Jawahery,[43] D. A. Roberts,[43] G. Simi,[43] J. M. Tuggle,[43] C. Dallapiccola,[44] E. Salvati,[44] S. Saremi,[44] R. Cowan,[45] D. Dujmic,[45] P. H. Fisher,[45] S. W. Henderson,[45] G. Sciolla,[45] M. Spitznagel,[45] R. K. Yamamoto,[45] M. Zhao,[45] P. M. Patel,[46] S. H. Robertson,[46] M. Schram,[46] A. Lazzaro,[47a,47b] V. Lombardo,[47a] F. Palombo,[47a,47b] S. Stracka,[47b] J. M. Bauer,[48] L. Cremaldi,[48] R. Godang,[48,¶] R. Kroeger,[48] D. J. Summers,[48] H. W. Zhao,[48] M. Simard,[49] P. Taras,[49] H. Nicholson,[50] G. De Nardo,[51a,51b] L. Lista,[51a] D. Monorchio,[51a,51b] G. Onorato,[51a,51b] C. Sciacca,[51a,51b] G. Raven,[52] H. L. Snoek,[52] C. P. Jessop,[53] K. J. Knoepfel,[53] J. M. LoSecco,[53] W. F. Wang,[53] L. A. Corwin,[54] K. Honscheid,[54] H. Kagan,[54] R. Kass,[54] J. P. Morris,[54] A. M. Rahimi,[54] J. J. Regensburger,[54] S. J. Sekula,[54] Q. K. Wong,[54] N. L. Blount,[55] J. Brau,[55] R. Frey,[55] O. Igonkina,[55] J. A. Kolb,[55] M. Lu,[55] R. Rahmat,[55] N. B. Sinev,[55] D. Strom,[55] J. Strube,[55] E. Torrence,[55] G. Castelli,[56a,56b] N. Gagliardi,[56a,56b] M. Margoni,[56a,56b] M. Morandin,[56a] M. Posocco,[56a] M. Rotondo,[56a] F. Simonetto,[56a,56b] R. Stroili,[56a,56b] C. Voci,[56a,56b] P. del Amo Sanchez,[57] E. Ben-Haim,[57] H. Briand,[57] J. Chauveau,[57] O. Hamon,[57] Ph. Leruste,[57] J. Ocariz,[57] A. Perez,[57] J. Prendki,[57] S. Sitt,[57] L. Gladney,[58] M. Biasini,[59a,59b] E. Manoni,[59a,59b] C. Angelini,[60a,60b] G. Batignani,[60a,60b] S. Bettarini,[60a,60b] G. Calderini,[60a,60b,**] M. Carpinelli,[60a,60b,††] A. Cervelli,[60a,60b] F. Forti,[60a,60b] M. A. Giorgi,[60a,60b] A. Lusiani,[60a,60c] G. Marchiori,[60a,60b] M. Morganti,[60a,60b] N. Neri,[60a,60b] E. Paoloni,[60a,60b] G. Rizzo,[60a,60b] J. J. Walsh,[60a] D. Lopes Pegna,[61] C. Lu,[61] J. Olsen,[61] A. J. S. Smith,[61] A. V. Telnov,[61] F. Anulli,[62a] E. Baracchini,[62a,62b] G. Cavoto,[62a] R. Faccini,[62a,62b] F. Ferrarotto,[62a] F. Ferroni,[62a,62b] M. Gaspero,[62a,62b] P. D. Jackson,[62a] L. Li Gioi,[62a] M. A. Mazzoni,[62a] S. Morganti,[62a] G. Piredda,[62a] F. Renga,[62a,62b] C. Voena,[62a] M. Ebert,[63] T. Hartmann,[63] H. Schröder,[63] R. Waldi,[63] T. Adye,[64] B. Franek,[64] E. O. Olaiya,[64] F. F. Wilson,[64] S. Emery,[65] L. Esteve,[65] G. Hamel de Monchenault,[65] W. Kozanecki,[65] G. Vasseur,[65] Ch. Yèche,[65] M. Zito,[65] X. R. Chen,[66] H. Liu,[66] W. Park,[66] M. V. Purohit,[66] R. M. White,[66] J. R. Wilson,[66] M. T. Allen,[67] D. Aston,[67] R. Bartoldus,[67] J. F. Benitez,[67] R. Cenci,[67] J. P. Coleman,[67] M. R. Convery,[67]

J. C. Dingfelder,[67] J. Dorfan,[67] G. P. Dubois-Felsmann,[67] W. Dunwoodie,[67] R. C. Field,[67] A. M. Gabareen,[67] M. T. Graham,[67] P. Grenier,[67] C. Hast,[67] W. R. Innes,[67] J. Kaminski,[67] M. H. Kelsey,[67] H. Kim,[67] P. Kim,[67] M. L. Kocian,[67] D. W. G. S. Leith,[67] S. Li,[67] B. Lindquist,[67] S. Luitz,[67] V. Luth,[67] H. L. Lynch,[67] D. B. MacFarlane,[67] H. Marsiske,[67] R. Messner,[67,*] D. R. Muller,[67] H. Neal,[67] S. Nelson,[67] C. P. O'Grady,[67] I. Ofte,[67] M. Perl,[67] B. N. Ratcliff,[67] A. Roodman,[67] A. A. Salnikov,[67] R. H. Schindler,[67] J. Schwiening,[67] A. Snyder,[67] D. Su,[67] M. K. Sullivan,[67] K. Suzuki,[67] S. K. Swain,[67] J. M. Thompson,[67] J. Va'vra,[67] A. P. Wagner,[67] M. Weaver,[67] C. A. West,[67] W. J. Wisniewski,[67] M. Wittgen,[67] D. H. Wright,[67] H. W. Wulsin,[67] A. K. Yarritu,[67] K. Yi,[67] C. C. Young,[67] V. Ziegler,[67] P. R. Burchat,[68] A. J. Edwards,[68] T. S. Miyashita,[68] S. Ahmed,[69] M. S. Alam,[69] J. A. Ernst,[69] B. Pan,[69] M. A. Saeed,[69] S. B. Zain,[69] S. M. Spanier,[70] B. J. Wogsland,[70] R. Eckmann,[71] J. L. Ritchie,[71] A. M. Ruland,[71] C. J. Schilling,[71] R. F. Schwitters,[71] B. W. Drummond,[72] J. M. Izen,[72] X. C. Lou,[72] F. Bianchi,[73a,73b] D. Gamba,[73a,73b] M. Pelliccioni,[73a,73b] M. Bomben,[74a,74b] L. Bosisio,[74a,74b] C. Cartaro,[74a,74b] G. Della Ricca,[74a,74b] L. Lanceri,[74a,74b] L. Vitale,[74a,74b] V. Azzolini,[75] N. Lopez-March,[75] F. Martinez-Vidal,[75] D. A. Milanes,[75] A. Oyanguren,[75] J. Albert,[76] Sw. Banerjee,[76] B. Bhuyan,[76] H. H. F. Choi,[76] K. Hamano,[76] G. J. King,[76] R. Kowalewski,[76] M. J. Lewczuk,[76] I. M. Nugent,[76] J. M. Roney,[76] R. J. Sobie,[76] T. J. Gershon,[77] P. F. Harrison,[77] J. Ilic,[77] T. E. Latham,[77] G. B. Mohanty,[77] E. M. T. Puccio,[77] H. R. Band,[78] X. Chen,[78] S. Dasu,[78] K. T. Flood,[78] Y. Pan,[78] R. Prepost,[78] C. O. Vuosalo,[78] and S. L. Wu[78]

(*BABAR* Collaboration)

[1]*Laboratoire d'Annecy-le-Vieux de Physique des Particules (LAPP), Université de Savoie, CNRS/IN2P3, F-74941 Annecy-Le-Vieux, France*
[2]*Universitat de Barcelona, Facultat de Fisica, Departament ECM, E-08028 Barcelona, Spain*
[3a]*INFN Sezione di Bari, I-70126 Bari, Italy*
[3b]*Dipartmento di Fisica, Università di Bari, I-70126 Bari, Italy*
[4]*University of Bergen, Institute of Physics, N-5007 Bergen, Norway*
[5]*Lawrence Berkeley National Laboratory and University of California, Berkeley, California 94720, USA*
[6]*University of Birmingham, Birmingham, B15 2TT, United Kingdom*
[7]*Ruhr Universität Bochum, Institut für Experimentalphysik 1, D-44780 Bochum, Germany*
[8]*University of British Columbia, Vancouver, British Columbia, Canada V6T 1Z1*
[9]*Brunel University, Uxbridge, Middlesex UB8 3PH, United Kingdom*
[10]*Budker Institute of Nuclear Physics, Novosibirsk 630090, Russia*
[11]*University of California at Irvine, Irvine, California 92697, USA*
[12]*University of California at Los Angeles, Los Angeles, California 90024, USA*
[13]*University of California at Riverside, Riverside, California 92521, USA*
[14]*University of California at San Diego, La Jolla, California 92093, USA*
[15]*University of California at Santa Barbara, Santa Barbara, California 93106, USA*
[16]*University of California at Santa Cruz, Institute for Particle Physics, Santa Cruz, California 95064, USA*
[17]*California Institute of Technology, Pasadena, California 91125, USA*
[18]*University of Cincinnati, Cincinnati, Ohio 45221, USA*
[19]*University of Colorado, Boulder, Colorado 80309, USA*
[20]*Colorado State University, Fort Collins, Colorado 80523, USA*
[21]*Technische Universität Dortmund, Fakultät Physik, D-44221 Dortmund, Germany*
[22]*Technische Universität Dresden, Institut für Kern- und Teilchenphysik, D-01062 Dresden, Germany*
[23]*Laboratoire Leprince-Ringuet, CNRS/IN2P3 , Ecole Polytechnique, F-91128 Palaiseau, France*
[24]*University of Edinburgh, Edinburgh EH9 3JZ, United Kingdom*
[25a]*INFN Sezione di Ferrara, I-44100 Ferrara, Italy*
[25b]*Dipartimento di Fisica, Università di Ferrara, I-44100 Ferrara, Italy*
[26]*INFN Laboratori Nazionali di Frascati, I-00044 Frascati, Italy*
[27a]*INFN Sezione di Genova, I-16146 Genova, Italy*
[27b]*Dipartimento di Fisica, Università di Genova, I-16146 Genova, Italy*
[28]*Harvard University, Cambridge, Massachusetts 02138, USA*
[29]*Universität Heidelberg, Physikalisches Institut, Philosophenweg 12, D-69120 Heidelberg, Germany*
[30]*Humboldt-Universität zu Berlin, Institut für Physik, Newtonstr. 15, D-12489 Berlin, Germany*
[31]*Imperial College London, London, SW7 2AZ, United Kingdom*
[32]*University of Iowa, Iowa City, Iowa 52242, USA*
[33]*Iowa State University, Ames, Iowa 50011-3160, USA*
[34]*Johns Hopkins University, Baltimore, Maryland 21218, USA*

[35]*Laboratoire de l'Accélérateur Linéaire, IN2P3/CNRS et Université Paris-Sud 11, Centre Scientifique d'Orsay, B. P. 34, F-91898 Orsay Cedex, France*
[36]*Lawrence Livermore National Laboratory, Livermore, California 94550, USA*
[37]*University of Liverpool, Liverpool L69 7ZE, United Kingdom*
[38]*Queen Mary, University of London, London, E1 4NS, United Kingdom*
[39]*University of London, Royal Holloway and Bedford New College, Egham, Surrey TW20 0EX, United Kingdom*
[40]*University of Louisville, Louisville, Kentucky 40292, USA*
[41]*Johannes Gutenberg-Universität Mainz, Institut für Kernphysik, D-55099 Mainz, Germany*
[42]*University of Manchester, Manchester M13 9PL, United Kingdom*
[43]*University of Maryland, College Park, Maryland 20742, USA*
[44]*University of Massachusetts, Amherst, Massachusetts 01003, USA*
[45]*Massachusetts Institute of Technology, Laboratory for Nuclear Science, Cambridge, Massachusetts 02139, USA*
[46]*McGill University, Montréal, Québec, Canada H3A 2T8*
[47a]*INFN Sezione di Milano, I-20133 Milano, Italy*
[47b]*Dipartimento di Fisica, Università di Milano, I-20133 Milano, Italy*
[48]*University of Mississippi, University, Mississippi 38677, USA*
[49]*Université de Montréal, Physique des Particules, Montréal, Québec, Canada H3C 3J7*
[50]*Mount Holyoke College, South Hadley, Massachusetts 01075, USA*
[51a]*INFN Sezione di Napoli, I-80126 Napoli, Italy*
[51b]*Dipartimento di Scienze Fisiche, Università di Napoli Federico II, I-80126 Napoli, Italy*
[52]*NIKHEF, National Institute for Nuclear Physics and High Energy Physics, NL-1009 DB Amsterdam, The Netherlands*
[53]*University of Notre Dame, Notre Dame, Indiana 46556, USA*
[54]*Ohio State University, Columbus, Ohio 43210, USA*
[55]*University of Oregon, Eugene, Oregon 97403, USA*
[56a]*INFN Sezione di Padova, I-35131 Padova, Italy*
[56b]*Dipartimento di Fisica, Università di Padova, I-35131 Padova, Italy*
[57]*Laboratoire de Physique Nucléaire et de Hautes Energies, IN2P3/CNRS, Université Pierre et Marie Curie-Paris6, Université Denis Diderot-Paris7, F-75252 Paris, France*
[58]*University of Pennsylvania, Philadelphia, Pennsylvania 19104, USA*
[59a]*INFN Sezione di Perugia, I-06100 Perugia, Italy*
[59b]*Dipartimento di Fisica, Università di Perugia, I-06100 Perugia, Italy*
[60a]*INFN Sezione di Pisa, I-56127 Pisa, Italy*
[60b]*Dipartimento di Fisica, Università di Pisa, I-56127 Pisa, Italy*
[60c]*Scuola Normale Superiore di Pisa, I-56127 Pisa, Italy*
[61]*Princeton University, Princeton, New Jersey 08544, USA*
[62a]*INFN Sezione di Roma, I-00185 Roma, Italy*
[62b]*Dipartimento di Fisica, Università di Roma La Sapienza, I-00185 Roma, Italy*
[63]*Universität Rostock, D-18051 Rostock, Germany*
[64]*Rutherford Appleton Laboratory, Chilton, Didcot, Oxon, OX11 0QX, United Kingdom*
[65]*CEA, Irfu, SPP, Centre de Saclay, F-91191 Gif-sur-Yvette, France*
[66]*University of South Carolina, Columbia, South Carolina 29208, USA*
[67]*SLAC National Accelerator Laboratory, Stanford, California 94309, USA*
[68]*Stanford University, Stanford, California 94305-4060, USA*
[69]*State University of New York, Albany, New York 12222, USA*
[70]*University of Tennessee, Knoxville, Tennessee 37996, USA*
[71]*University of Texas at Austin, Austin, Texas 78712, USA*
[72]*University of Texas at Dallas, Richardson, Texas 75083, USA*
[73a]*INFN Sezione di Torino, I-10125 Torino, Italy*
[73b]*Dipartimento di Fisica Sperimentale, Università di Torino, I-10125 Torino, Italy*
[74a]*INFN Sezione di Trieste, I-34127 Trieste, Italy*
[74b]*Dipartimento di Fisica, Università di Trieste, I-34127 Trieste, Italy*

[*]Deceased.
[†]Now at Temple University, Philadelphia, PA 19122, USA.
[‡]Now at Tel Aviv University, Tel Aviv, 69978, Israel.
[§]Also with Università di Perugia, Dipartimento di Fisica, Perugia, Italy.
[‖]Also with Università di Roma La Sapienza, I-00185 Roma, Italy.
[¶]Now at University of South Alabama, Mobile, AL 36688, USA.
[**]Also with Laboratoire de Physique Nucléaire et de Hautes Energies, IN2P3/CNRS, Université Pierre et Marie Curie-Paris 6, Université Denis Diderot-Paris7, F-75252 Paris, France.
[††]Also with Università di Sassari, Sassari, Italy.

[75]*IFIC, Universitat de Valencia-CSIC, E-46071 Valencia, Spain*
[76]*University of Victoria, Victoria, British Columbia, Canada V8W 3P6*
[77]*Department of Physics, University of Warwick, Coventry CV4 7AL, United Kingdom*
[78]*University of Wisconsin, Madison, Wisconsin 53706, USA*
(Received 10 February 2009; published 29 April 2009)

We present updated measurements of time-dependent *CP* asymmetries in fully reconstructed neutral B decays containing a charmonium meson. The measurements reported here use a data sample of $(465 \pm 5) \times 10^6$ $\Upsilon(4S) \to B\bar{B}$ decays collected with the *BABAR* detector at the PEP-II asymmetric energy e^+e^- storage rings operating at the SLAC National Accelerator Laboratory. The time-dependent *CP* asymmetry parameters measured from $J/\psi K^0_S$, $J/\psi K^0_L$, $\psi(2S)K^0_S$, $\eta_c K^0_S$, $\chi_{c1}K^0_S$, and $J/\psi K^*(892)^0$ decays are: $C_f = 0.024 \pm 0.020(\text{stat}) \pm 0.016(\text{syst})$ and $-\eta_f S_f = 0.687 \pm 0.028(\text{stat}) \pm 0.012(\text{syst})$.

DOI: 10.1103/PhysRevD.79.072009 PACS numbers: 13.25.Hw, 11.30.Er, 12.15.Hh

I. INTRODUCTION

The standard model (SM) of electroweak interactions describes *CP* violation as a consequence of an irreducible phase in the three-family Cabibbo-Kobayashi-Maskawa (CKM) quark-mixing matrix [1]. In the CKM framework, tree-diagram processes dominate neutral B decays to *CP* eigenstates containing a charmonium and a $K^{(*)0}$ meson. These provide a direct measurement of $\sin 2\beta$ [2], where the angle β is defined in terms of the CKM matrix elements V_{ij} for quarks i, j as $\arg[-(V_{cd}V^*_{cb})/(V_{td}V^*_{tb})]$.

We identify (tag) the initial flavor of the reconstructed B candidate, B_{rec}, using information from the other B meson, B_{tag}, in the event. The decay rate $g_+(g_-)$ for a neutral B meson to a *CP* eigenstate f accompanied by a $B^0(\bar{B}^0)$ tag, before taking into account detector resolution effect, can be expressed as

$$g_\pm(\Delta t) = \frac{e^{-|\Delta t|/\tau_{B^0}}}{4\tau_{B^0}}\{(1 \mp \Delta w) \pm (1 - 2w) \times [S_f \sin(\Delta m_d \Delta t) - C_f \cos(\Delta m_d \Delta t)]\}, \quad (1)$$

where

$$S_f = \frac{2\mathcal{I}m\lambda_f}{1 + |\lambda_f|^2}, \qquad C_f = \frac{1 - |\lambda_f|^2}{1 + |\lambda_f|^2},$$

$\Delta t \equiv t_{\text{rec}} - t_{\text{tag}}$ is the difference between the proper decay times of B_{rec} and B_{tag}, τ_{B^0} is the neutral B lifetime, and Δm_d is the mass difference between the B meson mass eigenstates determined from B^0-$\bar{B}^0$ oscillations [3]. Here, $\lambda_f = (q/p)(\bar{A}_f/A_f)$ [4], where q and p are complex constants that relate the B-meson flavor eigenstates to the mass eigenstates, and $\bar{A}_f/A_f$ is the ratio of the $\bar{B}^0$ and B^0 decay amplitudes to the final state f. We assume that the corresponding decay-width difference $\Delta\Gamma_d$ is zero. The average mistag probability w describes the effect of incorrect tags and Δw is the difference between the mistag probabilities for B^0 and $\bar{B}^0$ mesons. The sine term in Eq. (1) results from the interference between direct decay and decay after B^0-$\bar{B}^0$ oscillation. A nonzero cosine term arises from the interference between decay amplitudes with different weak and strong phases (direct *CP* violation $|\bar{A}_f/A_f| \neq 1$) or from *CP* violation in B^0-$\bar{B}^0$ mixing ($|q/p| \neq 1$). In the SM, *CP* violation in mixing and direct *CP* violation are both negligible in $b \to c\bar{c}s$ decays [4]. Under these assumptions, $\lambda_f = \eta_f e^{-2i\beta}$, where $\eta_f = +1(-1)$ is the *CP* eigenvalue for a *CP*-even (odd) final state, implying $C_f = 0$. Thus, the time-dependent *CP*-violating asymmetry is

$$A_{CP}(\Delta t) \equiv \frac{g_+(\Delta t) - g_-(\Delta t)}{g_+(\Delta t) + g_-(\Delta t)} = (1 - 2w)S_f \sin(\Delta m_d \Delta t), \quad (2)$$

and $S_f = -\eta_f \sin 2\beta$. If the assumption that $C_f = 0$ is relaxed, then $S_f = -\eta_f\sqrt{1 - C_f^2}\sin 2\beta$.

In a previous publication [5], we reported time-dependent *CP* asymmetries in terms of the parameters $\sin 2\beta$ and $|\lambda_f|$. In this paper, we report results in terms of S_f and C_f to be consistent with other time-dependent *CP* asymmetry measurements. We reconstruct B^0 decays to the final states $J/\psi K^0_S$, $J/\psi K^0_L$, $\psi(2S)K^0_S$, $\chi_{c1}K^0_S$, $\eta_c K^0_S$, and $J/\psi K^*(892)^0$ with $K^*(892)^0 \to K^0_S\pi^0$ [6]. The $J/\psi K^0_L$ final state is *CP*-even and the $J/\psi K^{*0}$ final state is an admixture of *CP*-even and *CP*-odd amplitudes. The remaining final states are *CP*-odd. The *CP*-even and odd amplitudes in $B^0 \to J/\psi K^{*0}$ decays can be separated in an angular analysis [7]. In this analysis, we average over the angular information resulting in a dilution of the measured *CP* asymmetry by a factor $1 - 2R_\perp$, where $R_\perp$ is the fraction of the $L = 1$ contribution. In Ref. [7] we have measured $R_\perp = 0.233 \pm 0.010(\text{stat}) \pm 0.005(\text{syst})$, which gives an effective $\eta_f = 0.504 \pm 0.033$ after acceptance corrections for $f = J/\psi K^{*0}$. In addition to measuring a combined S_f and C_f for the *CP* modes described above, we measure S_f and C_f for each final state f individually. We split the $J/\psi K^0_S$ mode into samples with either $K^0_S \to \pi^+\pi^-$ or $\pi^0\pi^0$. We also combined the $J/\psi K^0$ channel with K^0, either a K^0_S or K^0_L. Compared to our previous publication [5], the current analysis contains 82×10^6 additional $B\bar{B}$ decays and improved track reconstruction algorithms have been applied to the entire data set.

II. THE DATA SET AND *BABAR* DETECTOR

The results presented in this paper are based on data collected with the *BABAR* detector at the PEP-II asymmetric energy e^+e^- storage rings [8] operating at the SLAC National Accelerator Laboratory. At PEP-II, 9.0 GeV electrons and 3.1 GeV positrons collide at a center-of-mass energy of 10.58 GeV, which corresponds to the mass of the $\Upsilon(4S)$ resonance. The asymmetric energies result in a boost from the center-of-mass (CM) frame to the laboratory of $\beta\gamma \approx 0.56$. The data set analyzed has an integrated luminosity of 425.7 fb^{-1} corresponding to $(465 \pm 5) \times 10^6 B\bar{B}$ pairs recorded at the $\Upsilon(4S)$ resonance.

The *BABAR* detector is described in detail elsewhere [9]. Surrounding the interaction point is a five-layer, double-sided silicon vertex tracker (SVT), which measures the impact parameters of charged particle tracks in both the plane transverse to, and along the beam direction. A 40-layer drift chamber surrounds the silicon vertex tracker and provides measurements of the momenta for charged particles. Charged hadron identification is achieved through measurements of particle energy loss in the tracking system and the Cherenkov angle obtained from a detector of internally reflected Cherenkov light. A CsI(Tl) electromagnetic calorimeter (EMC) provides photon detection, electron identification, and π^0 reconstruction. The aforementioned components are enclosed by a solenoid magnet, which provides a 1.5 T magnetic field. Finally, the flux return of the magnet (IFR) is instrumented in order to allow discrimination of muons from pions. For the most recent 211.7 fb^{-1} of data, a portion of the resistive plate chambers in the IFR has been replaced by limited streamer tubes [10].

We use a right-handed coordinate system with the z axis along the electron beam direction and the y axis upward. Unless otherwise stated, kinematic quantities are calculated in the laboratory rest frame. We use Monte Carlo (MC) simulated events generated with the *BABAR* simulation based on GEANT4 [11] for detector responses and EvtGen [12] for event kinematics to determine signal and background characteristics, optimize selection criteria, and evaluate efficiencies.

III. RECONSTRUCTION OF *B* CANDIDATES

We select two samples of events in order to measure the time-dependent *CP* asymmetry parameters S_f and C_f: a sample of signal events used in the extraction of the *CP* parameters (B_{CP}) and a sample of fully reconstructed B meson decays to flavor eigenstates ($B_{\rm flav}$). The B_{CP} sample consists of B^0 decays to $J/\psi K^0_S$, $J/\psi K^0_L$, $\psi(2S)K^0_S$, $\eta_c K^0_S$, $\chi_{c1}K^0_S$, and $J/\psi K^*(892)^0$, where K^{*0} decays to $K^0_S\pi^0$. The $B_{\rm flav}$ sample consists of B^0 decays to $D^{(*)-}(\pi^+, \rho^+, a_1^+)$ final states. We use the $B_{\rm flav}$ sample to determine the dilution (mistag probability) and the resolution function, discussed in Sec. V. We assume that the interference between the *CP* side and the tag side reconstruction is negligible and therefore that the dilution and resolution parameters are the same for the $B_{\rm flav}$ and B_{CP} samples. We also select a sample of fully reconstructed charged B meson decays to $J/\psi K^+$, $\psi(2S)K^+$, $\chi_{c1}K^+$, $\eta_c K^+$, and $J/\psi K^*(892)^+$, where K^{*+} decays to $K^+\pi^0$ or $K^0_S\pi^+$, to use as a control sample.

The event selection is unchanged from that described in Ref. [5]. J/ψ and $\psi(2S)$ mesons are reconstructed via their decays to e^+e^- or $\mu^+\mu^-$ final states. At least one of the leptons is required to pass a likelihood particle identification algorithm based on the information provided by the EMC, the IFR, and from ionization energy loss measured in the tracking system. We require the invariant mass of the muon pair $m(\mu^+\mu^-)$ to be in the mass range 3.06–3.14 GeV/c^2 for J/ψ or 3.636–3.736 GeV/c^2 for $\psi(2S)$ candidates. For $J/\psi \to e^+e^-$ and $\psi(2S) \to e^+e^-$ decays, where the electron may have radiated bremsstrahlung photons, part of the missing energy is recovered by identifying neutral clusters with more than 30 MeV lying within 35 mrad in the polar angle and 50 mrad in azimuth of the electron direction projected onto the EMC. The invariant mass of e^+e^- pairs is required to be within 2.95–3.14 GeV/c^2 for J/ψ candidates, or 3.436–3.736 GeV/c^2 for $\psi(2S)$ candidates.

We also construct $\psi(2S)$ mesons in the $J/\psi\pi^+\pi^-$ final state, where the J/ψ candidate is combined with a pair of oppositely-charged tracks assumed as pions with no particle identification applied, and the pion pair-invariant mass between 400 MeV/c^2 and 600 MeV/c^2. Candidates with $3.671\ \text{GeV}/c^2 < m(J/\psi\pi^+\pi^-) < 3.701\ \text{GeV}/c^2$ are retained.

The χ_{c1} candidates are reconstructed in the $J/\psi\gamma$ final state. The photon candidates are required to have an energy greater than 100 MeV but less than 2 GeV, and, when combined with other photons, not to form a π^0 candidate with invariant mass $120\ \text{MeV}/c^2 < m(\gamma\gamma) < 150\ \text{MeV}/c^2$. The invariant mass of the χ_{c1} candidate is required to be between 3.477 GeV/c^2 and 3.577 GeV/c^2. Mass constraints are applied in the fits to improve the determinations of the energies and momenta of the J/ψ, $\psi(2S)$, and χ_{c1} candidates.

We reconstruct the $B^0 \to \eta_c K^0_S$ mode using the $\eta_c \to K^0_S K^+\pi^-$ decay. We exploit the fact that the η_c decays predominantly through a $K\pi$ resonance at around 1.43 GeV/c^2 and a $K^0_S K$ resonance close to the threshold. We require that $m(K^0_S\pi^-)$ or $m(K^+\pi^-)$ is within the mass range of 1.26 GeV/c^2 and 1.63 GeV/c^2, or $1.0\ \text{GeV}/c^2 < m(K^+K^0_S) < 1.4\ \text{GeV}/c^2$.

The decay channels $K^+\pi^-$, $K^+\pi^-\pi^0$, $K^+\pi^+\pi^-\pi^-$, and $K^0_S\pi^+\pi^-$ are used to reconstruct $\bar{D}^0$, while D^- candidates are selected in the $K^+\pi^-\pi^-$ and $K^0_S\pi^-$ modes. We require that the $\bar{D}^0$ and D^- candidate invariant mass is within $\pm 3\sigma$ of their respective nominal mass, where σ is the uncertainty calculated for each candidate. A mass-

constrained fit is then applied to the $\bar{D}^0$ and D^- candidates satisfying these requirements. We form D^{*-} candidates in the decay $D^{*-} \to \bar{D}^0\pi^-$ by combining a $\bar{D}^0$ with a pion that has momentum greater than 70 MeV/c. The D^{*-} candidates are required to have $m(\bar{D}^0\pi^-)$ within ± 1.1 MeV/c^2 of the nominal D^{*-} mass for the $\bar{D}^0 \to K^+\pi^-\pi^0$ mode and ± 0.8 MeV/c^2 for all other modes.

For the $J/\psi K^0_S$ decay, we use both $K^0_S \to \pi^+\pi^-$ and $K^0_S \to \pi^0\pi^0$ decays; for other B decay modes we only use $K^0_S \to \pi^+\pi^-$. Candidates in the $K^0_S \to \pi^+\pi^-$ mode are selected by requiring an invariant $\pi^+\pi^-$ mass, computed at the vertex of the two oppositely-charged tracks, between 472.67 MeV/c^2 and 522.67 MeV/c^2. We further apply a mass constraint fit to the K^0_S candidates before combining them with charmonium candidates to form B^0 candidates. Neutral pion candidates, in the mass range 100–155 MeV/c^2, are formed from two γ candidates from the EMC. Pairs of π^0 are combined to construct $K^0_S \to \pi^0\pi^0$ candidates. The minimum energy is required to be 30 MeV for γ, 200 MeV for π^0, and 800 MeV for K^0_S candidates. To select K^0_S candidates, the $\pi^0\pi^0$ invariant mass is restricted to the region between 470 MeV/c^2 and 550 MeV/c^2.

Candidates for K^0_L are identified in the EMC and IFR detectors as reconstructed clusters that cannot be associated with any charged track in the event. As the energy of K^0_L cannot be measured well, the laboratory momentum of the K^0_L is determined by its flight direction and the constraint that the invariant mass of the $J/\psi K^0_L$ system has the known B^0 mass. For events with multiple $J/\psi K^0_L$ candidates, a hierarchy is imposed where the highest energy EMC cluster for multiple EMC combinations, or the IFR cluster with the largest number of layers for multiple IFR combinations, is selected. In case both EMC and IFR combinations are found, the EMC combination is chosen because of its better angular resolution.

We reconstruct K^{*0} candidates in the $K^0_S\pi^0$ mode, while K^{*+} candidates are reconstructed in the $K^+\pi^0$ and $K^0_S\pi^+$ modes. The invariant mass of the two daughters is required to be within ± 100 MeV/c^2 of the nominal K^* mass.

The ρ^+ candidates are reconstructed in the $\pi^+\pi^0$ final state, where the $\pi^+\pi^0$ mass is required to lie within ± 150 MeV/c^2 of the nominal ρ^+ mass. Candidates in the decay mode $a_1^+ \to \pi^+\pi^-\pi^+$ are reconstructed by combining three charged tracks with pion mass assumption, and restricting the three-pion invariant mass to lie between 1.0 and 1.6 GeV/c^2.

Events that pass the selection requirements are refined using kinematic variables. For the $J/\psi K^0_L$ mode, the difference ΔE between the candidate's CM energy and the beam energy in the CM frame, $E^*_{\rm beam}$, is required to satisfy $|\Delta E| < 80$ MeV. For all other categories of events, we require $|\Delta E| < 20$ MeV and the beam-energy substituted mass $m_{\rm ES} = \sqrt{(E^*_{\rm beam})^2 - (p^*_B)^2}$ to be greater than 5.2 GeV/c^2, where p^*_B is the B momentum in the CM frame. When multiple B candidates (with $m_{\rm ES} > 5.2$ GeV/c^2) are found in the same event, the candidate with the smallest value of $|\Delta E|$ is selected.

We calculate the proper time difference Δt between the two B decays from the measured separation Δz between the decay vertices of $B_{\rm rec}$ and $B_{\rm tag}$ along the collision (z) axis [13]. The z position of the $B_{\rm rec}$ vertex is determined from the charged daughter tracks. The $B_{\rm tag}$ decay vertex is determined by fitting tracks not belonging to the $B_{\rm rec}$ candidate to a common vertex, including constraints from the beam spot location and the $B_{\rm rec}$ momentum [13]. Events are accepted if the calculated Δt uncertainty is less than 2.5 ps and $|\Delta t|$ is less than 20 ps. The fraction of signal MC events satisfying such a requirement is 95%.

IV. *B* MESON FLAVOR TAGGING

A key ingredient in the measurement of time-dependent CP asymmetries is the determination of whether the $B_{\rm rec}$ was a B^0 or a $\bar{B}^0$ at the time of $\Delta t = 0$. This ''flavor tagging'' is achieved with the analysis of the decay products of the recoiling B meson $B_{\rm tag}$. The overwhelming majority of B mesons decay to a final state that is flavor-specific, i.e., only accessible from either a B^0 or a $\bar{B}^0$. The purpose of the flavor-tagging algorithm is to determine the flavor of $B_{\rm tag}$ with the highest efficiency $\epsilon_{\rm tag}$ and lowest probability w of assigning the wrong flavor. It is not necessary to fully reconstruct $B_{\rm tag}$ in order to determine its flavor.

The figure of merit for the performance of the tagging algorithm is the effective tagging efficiency

$$Q = \epsilon_{\rm tag}(1-2w)^2, \tag{3}$$

which is related to the statistical uncertainty σ_S and σ_C in the coefficients S_f and C_f through

$$\sigma_{S,C} \propto \frac{1}{\sqrt{Q}}. \tag{4}$$

The tagging algorithm we employ [5,13] analyzes tracks on the tag side to assign a flavor and associated probability to $B_{\rm tag}$. The flavor of $B_{\rm tag}$ is determined from a combination of nine different tag signatures, such as isolated primary leptons, kaons, and pions from B decays to final states containing D^* mesons, and high momentum charged particles from B decays. The properties of those signatures are used as inputs to a single neural network that is trained to assign the correct flavor to $B_{\rm tag}$. The output of this neural network then is divided into seven mutually exclusive categories. These are (in order of decreasing signal purity) *Lepton, Kaon I, Kaon II, KaonPion, Pion, Other*, and *Notag*. The events with the neural network output $|NN| > 0.8$ are defined as a *Lepton* category, if they are also accompanied by an isolated primary lepton; otherwise they are categorized as a *Kaon I* tag. For the other five tag categories (*Kaon II, KaonPion, Pion, Other*, and

TABLE I. Efficiencies ϵ_i, average mistag fractions w_i, mistag fraction differences between B^0 and $\bar{B}^0$ tagged events Δw_i, and effective tagging efficiency Q_i extracted for each tagging category i from the $B_{\rm flav}$ sample.

Category	ϵ_i (%)	w_i (%)	Δw_i (%)	Q_i (%)
Lepton	8.96 ± 0.07	2.8 ± 0.3	0.3 ± 0.5	7.98 ± 0.11
Kaon I	10.82 ± 0.07	5.3 ± 0.3	-0.1 ± 0.6	8.65 ± 0.14
Kaon II	17.19 ± 0.09	14.5 ± 0.3	0.4 ± 0.6	8.68 ± 0.17
KaonPion	13.67 ± 0.08	23.3 ± 0.4	-0.7 ± 0.7	3.91 ± 0.12
Pion	14.18 ± 0.08	32.5 ± 0.4	5.1 ± 0.7	1.73 ± 0.09
Other	9.54 ± 0.07	41.5 ± 0.5	3.8 ± 0.8	0.27 ± 0.04
All	74.37 ± 0.10			31.2 ± 0.3

Notag) the outputs of the neutral network are required to satisfy: $0.6 < |NN| < 0.8$, $0.4 < |NN| < 0.6$, $0.2 < |NN| < 0.4$, $0.1 < |NN| < 0.2$, and $|NN| < 0.1$, respectively.

The performance of this algorithm is evaluated using the $B_{\rm flav}$ sample. The final state of the $B_{\rm flav}$ sample can be classified as mixed or unmixed depending on whether the reconstructed flavor eigenstate $B_{\rm flav}$ has the same or opposite flavor as the tagging B. After taking the mistag probability into account, the decay rate $g_{\pm,B^0}$ ($g_{\pm,\bar{B}^0}$) for a neutral B meson to decay to a flavor eigenstate accompanied by a B^0 ($\bar{B}^0$) tag can be expressed as

$$\begin{aligned} g_{\pm,B^0}(\Delta t) &\propto [(1 - \Delta w_i) \pm (1 - 2w_i)\cos(\Delta m_d \Delta t)], \\ g_{\pm,\bar{B}^0}(\Delta t) &\propto [(1 + \Delta w_i) \pm (1 - 2w_i)\cos(\Delta m_d \Delta t)], \end{aligned} \quad (5)$$

where the $\pm$ sign in the index refers to mixed ($-$) and unmixed ($+$) events; the index i denotes the ith tagging category. The performance of the tagging algorithm is summarized in Table I. The events in the *Notag* category contain no flavor information, so carry no weight in the time-dependent analysis. They are excluded from further analysis. The total effective tagging efficiency is measured to be $(31.2 \pm 0.3)\%$.

V. LIKELIHOOD FIT METHOD

We determine the composition of our final sample by performing simultaneous fits to the $m_{\rm ES}$ distributions for the full B_{CP} and $B_{\rm flav}$ samples, except for the $J/\psi K^0_L$ sample for which we extract the K^0_L momentum by using the B^0 mass constraint and fit the ΔE distribution. We then perform a simultaneous maximum likelihood fit to the Δt distribution of the tagged B_{CP} and $B_{\rm flav}$ samples to measure S_f and C_f.

We define a signal region of $5.27 < m_{\rm ES} < 5.29$ GeV/c^2 ($|\Delta E| < 10$ MeV for $J/\psi K^0_L$), which contains 15 481 candidate events of a B_{CP} sample that satisfy the tagging and vertexing requirements (see Table II). The signal $m_{\rm ES}$ distribution for the full B_{CP} and $B_{\rm flav}$ samples, except for the $J/\psi K^0_L$ sample, is described by a Gaussian function. The background $m_{\rm ES}$ distribution is modeled by an ARGUS threshold function [14], where a shape parameter is allowed to vary in the fit. For the decay modes of $J/\psi K^0_S$, $\psi 2s K^0_S$, $\chi_{c1} K^0_S$, $J/\psi K^{*0}$, and $B_{\rm flav}$, we use simulated events to estimate the fractions of background events that peak in the $m_{\rm ES}$ signal region ($m_{\rm ES} > 5.27$ GeV/c^2) due to cross feed from other decay modes. We describe this component with a Gaussian function having the same mean and width as the signal and refer to it as the peaking background because if neglected, it would lead to an overestimate of the signal yield. The peaking background is less than 1% in the decay of $B^0 \to J/\psi K^0_S$, and at the level of a few percent in most other decay modes. The only exception is the decay of $B^0 \to J/\psi K^{*0}$, where the peaking background level is about 13%. MC simulations show that it consists of 44% of B^+ decays, 32% of $B^0 \to \chi_c K^0_S$ decays, and 24% of other B^0 decays. For the $\eta_c K^0_S$ mode, the cross feed fraction is determined from a fit to the $m_{KK\pi}$ and $m_{\rm ES}$ distributions in data. For the $J/\psi K^0_L$ decay mode, the signal ΔE distribution is determined from MC simulated events. The sample composition, effective η_f, and ΔE distribution of the individual background sources are determined either from simulation (for $B \to J/\psi X$) or from the $m_{\ell^+\ell^-}$ sidebands in data (for non-J/ψ background). Figure 1 shows the distributions of $m_{\rm ES}$ obtained

TABLE II. Number of events $N_{\rm tag}$ and signal purity P in the signal region after tagging and vertexing requirements, and results of fitting for *CP* asymmetries in the B_{CP} sample and various subsamples. Fit results for the $B_{\rm flav}$ and B^+ control samples are also shown here. Errors are statistical only.

Sample	$N_{\rm tag}$	P (%)	$-\eta_f S_f$	C_f
Full *CP* sample	15 481	76	0.687 ± 0.028	0.024 ± 0.020
$J/\psi K^0_S(\pi^+\pi^-)$	5426	96	0.662 ± 0.039	0.017 ± 0.028
$J/\psi K^0_S(\pi^0\pi^0)$	1324	87	0.625 ± 0.091	0.091 ± 0.063
$\psi(2S)K^0_S$	861	87	0.897 ± 0.100	0.089 ± 0.076
$\chi_{c1}K^0_S$	385	88	0.614 ± 0.160	0.129 ± 0.109
$\eta_c K^0_S$	381	79	0.925 ± 0.160	0.080 ± 0.124
$J/\psi K^0_L$	5813	56	0.694 ± 0.061	-0.033 ± 0.050
$J/\psi K^{*0}$	1291	67	0.601 ± 0.239	0.025 ± 0.083
$J/\psi K^0_S$	6750	95	0.657 ± 0.036	0.026 ± 0.025
$J/\psi K^0$	12 563	77	0.666 ± 0.031	0.016 ± 0.023
$\eta_f = -1$	8377	93	0.684 ± 0.032	0.037 ± 0.023
1999–2002 data	3079	78	0.732 ± 0.061	0.020 ± 0.045
2003–2004 data	4916	77	0.720 ± 0.050	0.045 ± 0.036
2005–2006 data	4721	76	0.632 ± 0.052	0.027 ± 0.037
2007 data	2765	75	0.663 ± 0.071	-0.023 ± 0.049
Lepton	1740	83	0.732 ± 0.052	0.074 ± 0.038
Kaon I	2187	78	0.615 ± 0.053	-0.046 ± 0.039
Kaon II	3630	76	0.688 ± 0.056	0.068 ± 0.039
KaonPion	2882	74	0.741 ± 0.086	0.013 ± 0.061
Pion	3053	76	0.711 ± 0.132	0.016 ± 0.090
Other	1989	74	0.766 ± 0.347	-0.176 ± 0.236
$B_{\rm flav}$ sample	166 276	83	0.021 ± 0.009	0.012 ± 0.006
B^+ sample	36 082	94	0.021 ± 0.016	0.013 ± 0.011

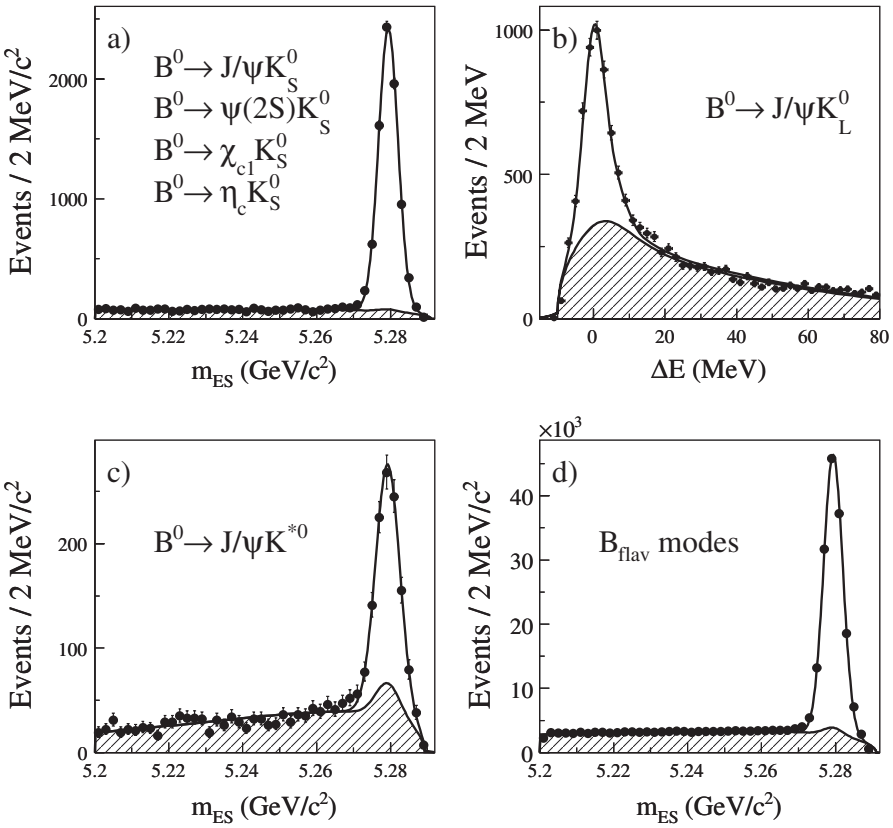

FIG. 1. Distributions for B_{CP} and $B_{\rm flav}$ candidates satisfying the tagging and vertexing requirements: (a) $m_{\rm ES}$ for the final states $J/\psi K^0_S$, $\psi(2S)K^0_S$, $\chi_{c1}K^0_S$, and $\eta_c K^0_S$; (b) ΔE for the final state $J/\psi K^0_L$; (c) $m_{\rm ES}$ for $J/\psi K^{*0}(K^{*0} \to K^0_S\pi^0)$; and (d) $m_{\rm ES}$ for the $B_{\rm flav}$ sample. In each plot, the shaded region is the estimated background contribution.

for the B_{CP} and $B_{\rm flav}$ events, and ΔE obtained for the $J/\psi K^0_L$ events.

The Δt distributions of the B_{CP} sample are modeled by Eq. (1) and those of the $B_{\rm flav}$ sample by Eq. (5). The Δt distributions for the signal are convolved with a resolution function common to both the $B_{\rm flav}$ and B_{CP} samples, modeled by the sum of three Gaussian functions [13], called the core, tail, and outlier components, which can be represented as a function of the reconstruction uncertainty $\delta t = \Delta t - \Delta t_{\rm true}$ as follows:

$$\begin{aligned}\mathcal{R}(\delta t; \sigma_{\Delta t}) = {} & f_{\rm core} h_G(\delta t; \delta_{\rm core}\sigma_{\Delta t}, S_{\rm core}\sigma_{\Delta t}) \\ & + f_{\rm tail} h_G(\delta t; \delta_{\rm tail}\sigma_{\Delta t}, S_{\rm tail}\sigma_{\Delta t}) \\ & + f_{\rm out} h_G(\delta t; \delta_{\rm out}, S_{\rm out}),\end{aligned} \tag{6}$$

where

$$h_G(\delta t; \delta, \sigma) = \frac{1}{\sqrt{2\pi}\sigma} \exp\left(-\frac{(\delta t - \delta)^2}{2\sigma^2}\right), \tag{7}$$

and

$$f_{\rm core} + f_{\rm tail} + f_{\rm out} = 1. \tag{8}$$

The widths (σ) of the core and tail components include two independent scale factors, $S_{\rm core}$ and $S_{\rm tail}$, to accommodate an overall underestimate or overestimate of the Δt measurement error $\sigma_{\Delta t}$ for all events. The parameter $S_{\rm core}$ is free in the fit and its value is close to unity. The value of $S_{\rm tail}$ is derived from MC studies and fixed to be 3. Studies show that the measurement of C_f and S_f is not sensitive to the choice of the $S_{\rm tail}$ value. We later vary the $S_{\rm tail}$ value within a large region and assign the shift of the measured C_f and S_f values as the corresponding systematic uncertainties. We account for residual charm decay products included in the $B_{\rm tag}$ candidate vertex by allowing the core and tail Gaussian functions to have nonzero mean values (bias, $\delta_{\rm core} \neq 0$ and $\delta_{\rm tail} \neq 0$). The bias ($\delta_{\rm core}$) and width ($S_{\rm core}$) of the core component are allowed to differ for the lepton-tagged and nonlepton-tagged events. We use common parameters for the tail component. In order to account for the strong correlations with other resolution parameters, the outlier component bias ($\delta_{\rm out}$) and width ($S_{\rm out}$) are fixed to 0 ps and 8 ps, respectively.

The Δt spectrum of the combinatorial background is described by an empirical distribution, consisting of components with zero and nonzero lifetimes ($\tau_{\rm bg}$) that are convolved with a resolution function [13] distinct from that used for the signal. Here, we use a double-Gaussian distribution, which has components similar to the core and

outlier distributions described above. In this case, the resolution function is common to all tagging categories. The peaking background is assigned the same Δt distribution as the signal but with $S_f = C_f = 0$, and uses the same Δt resolution function as the signal. The nonzero lifetime component of the combinatorial background contains both mixed and unmixed events. Therefore, we allow the value of Δm_d for this component ($\Delta m_{d,\mathrm{bg}}$) to vary in the fit.

In addition to S_f and C_f, there are 69 free parameters in the fit. For the signal, these are

(i) 7 parameters for the Δt resolution: δ_{core} and S_{core} for the lepton-tagged and nonlepton-tagged events, f_{core}, f_{tail}, and δ_{tail};
(ii) 12 parameters for the average mistag fractions w_i and the differences Δw_i between B^0 and $\bar{B}^0$ mistag fractions for each tagging category;
(iii) 1 parameter for the small difference between B^0 and $\bar{B}^0$ reconstruction efficiency [13]; and
(iv) 6 parameters for the small difference between B^0 and $\bar{B}^0$ tagging efficiencies in each tagging category [13].

The background parameters that are allowed to vary are

(i) 24 mistag fraction parameters: w_i and Δw_i of each tagging category for background components with zero and nonzero lifetime, respectively;
(ii) 3 parameters for the Δt resolution: δ_{core}, S_{core}, and f_{core};
(iii) 4 parameters for the B_{flav} time dependence: 2 parameters for the fraction (f_{prompt}) of a zero lifetime component for the lepton-tagged and nonlepton-tagged events, τ_{bg} and $\Delta m_{d,\mathrm{bg}}$;
(iv) 8 parameters for possible *CP* violation in the background, including the apparent *CP* asymmetry of nonpeaking events in each tagging category;
(v) 1 parameter for possible direct *CP* violation in the $\chi_{c1}K^0_S$ background coming from $J/\psi K^{*0}$, and
(vi) 3 parameters for possible direct *CP* violation in the $J/\psi K^0_L$ mode, coming from $J/\psi K^0_S$, $J/\psi K^{*0}$, and the remaining J/ψ backgrounds.

The effective value of $|\lambda_f|$ for the non-J/ψ background is fixed from a fit to the J/ψ-candidate sidebands in $J/\psi K^0_L$. We fix $\tau_{B^0} = 1.530$ ps and $\Delta m_d = 0.507$ ps^{-1} [3]. The determination of the mistag fractions and Δt resolution function parameters for the signal is dominated by the B_{flav} sample, which is about 10 times larger than the *CP* sample.

VI. LIKELIHOOD FIT VALIDATION

We perform three tests to validate the fitting procedure. The first of these tests consists of generating ensembles of simulated experiments from the probability density function and fitting each simulated experiment. We determine that the fitted values of S_f and C_f parameters are unbiased, and that the fit returns reasonable estimates of the statistical uncertainties by verifying the distribution of the pull $\mathcal{P}$ on a parameter $\mathcal{O}$, given by $\mathcal{P} = (\mathcal{O}_{\mathrm{fit}} - \mathcal{O}_{\mathrm{gen}})/\sigma(\mathcal{O}_{\mathrm{fit}})$, is consistent with a Gaussian centered about zero with a width of one. The quantity $\mathcal{O}_{\mathrm{fit}}$ is the fitted value, with a fitted error of $\sigma(\mathcal{O}_{\mathrm{fit}})$, and $\mathcal{O}_{\mathrm{gen}}$ is the generated value.

The second test involves fitting simulated signal events that include the full *BABAR* detector simulation. For each decay mode, we divide the signal MC sample to many data-sized samples, fit them one by one, and then examine the distribution of the fitted results. We make sure that the $\mathcal{P}$ distributions for these signal-only simulated experiments are consistent with a Gaussian distribution centered at zero with a width of one.

The third test is to perform null tests on control samples of neutral and charged B events where S_f and C_f should be very small or zero. The parameters S_f and C_f are consistent with zero for the charged B sample of the $J/\psi K^{\pm}$, $\psi(2S)K^{\pm}$, $\chi_{c1}K^{\pm}$, and $J/\psi K^{*\pm}$ final states. For the neutral B_{flav} sample, we find that the S_f and C_f parameters slightly deviate from zero at approximately twice the statistical uncertainty (see Table II). The deviation of S_f from zero is consistent with the directly measured *CP* asymmetry $S \sim -2r\sin(2\beta+\gamma)\cos(\delta) \lesssim 0.04$ [15] in $B^0 \to D^{(*)\pm}h^{\mp}$ [16] due to interference from doubly CKM-suppressed decays, where $\gamma = \arg[-(V_{\mathrm{ud}}V^*_{\mathrm{ub}})/(V_{\mathrm{cd}}V^*_{\mathrm{cb}})]$, δ is the strong phase difference between CKM-favored and doubly CKM-suppressed amplitudes, and $r \sim 0.02$ is the ratio of the two amplitudes. Considering this expected *CP* asymmetry in the B_{flav} sample and systematic uncertainties (at $\sim$1% level), we conclude that our analysis is free of pathological behaviors.

VII. RESULTS

The fit to the B_{CP} and B_{flav} samples yields $-\eta_f S_f = 0.687 \pm 0.028$ and $C_f = 0.024 \pm 0.020$, where the errors are statistical only. The correlation between these two parameters is $+0.1\%$. We also performed the fit using $\sin 2\beta$ and $|\lambda_f|$ as fitted parameters, and found $\sin 2\beta = 0.687 \pm 0.028$ and $|\lambda_f| = 0.977 \pm 0.020$. The correlation between the fitted $\sin 2\beta$ and $|\lambda_f|$ parameters is -0.14%. Figure 2 shows the Δt distributions and asymmetries in yields between events with B^0 and $\bar{B}^0$ tags for the $\eta_f = -1$ and $\eta_f = +1$ samples as a function of Δt, overlaid with the projection of the likelihood fit result. Figure 3 shows the time-dependent asymmetry between unmixed and mixed events for hadronic B candidates with $m_{\mathrm{ES}} > 5.27$ GeV/c^2. We also perform a fit in which we allow different S_f and C_f values for each charmonium decay mode, a fit to the $J/\psi K^0_S(\pi^+\pi^- + \pi^0\pi^0)$ mode, and a fit to the $J/\psi K^0(K^0_S + K^0_L)$ sample. The results for some of these studies are shown in Fig. 4. We split the data sample by run period and by tagging category. We perform the *CP* measurements on control samples with no expected *CP* asymmetry. The results of these fits are summarized in Table II.

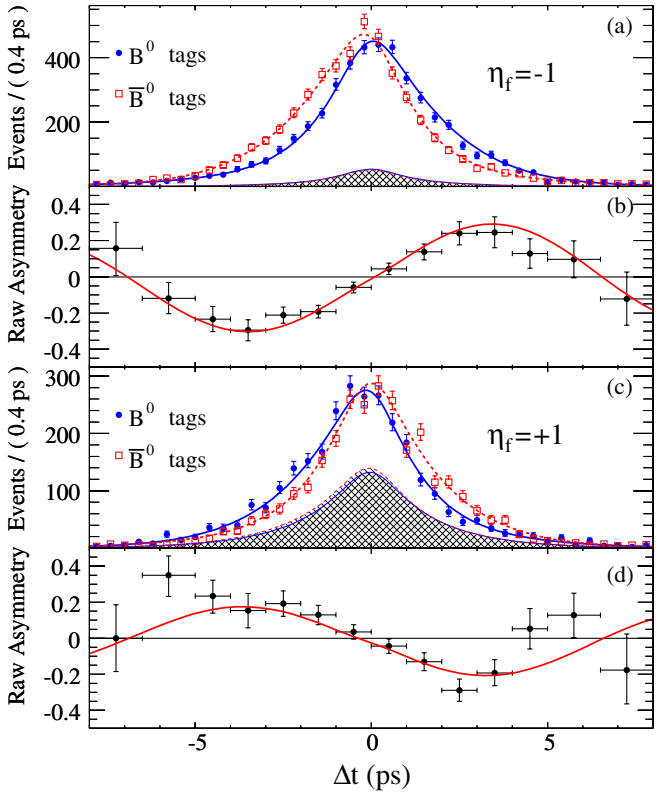

FIG. 2 (color online). (a) Number of $\eta_f = -1$ candidates ($J/\psi K_S^0$, $\psi(2S)K_S^0$, $\chi_{c1}K_S^0$, and $\eta_c K_S^0$) in the signal region with a B^0 tag (N_{B^0}) and with a $\bar{B}^0$ tag ($N_{\bar{B}^0}$); and (b) the raw asymmetry, $(N_{B^0} - N_{\bar{B}^0})/(N_{B^0} + N_{\bar{B}^0})$, as functions of Δt; (c) and (d) are the corresponding distributions for the $\eta_f = +1$ mode $J/\psi K_L^0$. The solid (dashed) curves in (a) and (c) represent the fit projections in Δt for $B^0(\bar{B}^0)$ tags. The shaded regions represent the estimated background contributions to (a) and (c). The curves in (b) and (d) are the fit projections of the raw asymmetry between B^0 tagged and $\bar{B}^0$ tagged events.

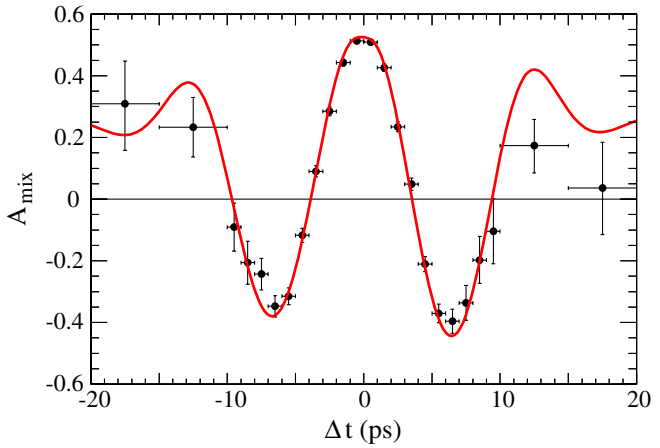

FIG. 3 (color online). Time-dependent asymmetry between unmixed and mixed events, $A_{\rm mix} = (N_{\rm unmix} - N_{\rm mix})/(N_{\rm unmix} + N_{\rm mix})$, as a function of Δt for hadronic B candidates ($B_{\rm flav}$) with $m_{\rm ES} > 5.27$ GeV/c^2. The curve is the corresponding fit projection.

The dominant systematic uncertainties on S_f are summarized in Tables III and IV. The dilution due to flavor tagging can be different between B_{CP} and $B_{\rm flav}$ events. We study this effect by comparing the results in large samples of simulated B_{CP} and $B_{\rm flav}$ events. The uncertainties due to Δt resolution functions for both signal and background components are estimated by varying the fixed parameters and by using alternative models. We also vary the peaking background fractions based on estimates derived from simulation, and vary the CP content of the background over a wide range to estimate the effect due to our limited knowledge of background properties. The uncertainties in the $J/\psi K_L^0$ sample are studied by varying the compositions of the signal and background, by modifying the ΔE probability density function based on studies performed with the $J/\psi K_S^0$ control sample, and by varying the branching fractions of the background modes and their CP asymmetries. Other sources of uncertainty such as the values of the physics parameters Δm_d, τ_B, $\Delta\Gamma_d/\Gamma_d$, the beam spot and detector alignment, and other fixed parameters, are studied by varying them according to their world averages, the calibration, and the statistical uncertainty, respectively. Despite the large amount of simulated signal events that included the full *BABAR* detector simulation, we can only validate the possible fit bias to be no more than certain precision. As a result, we assign a systematic uncertainty corresponding to any deviations and the statistical uncertainties of the mean values of the fitted S_f and C_f from the generated values as the possible fit bias (MC statistics).

The only sizable systematic uncertainties on C_f are due to the CP content of the peaking backgrounds and due to the possible interference between the suppressed $\bar{b} \to \bar{u}c\bar{d}$ amplitude with the favored $b \to c\bar{u}d$ amplitude for some tag-side B decays [15]. The total systematic error on $S_f(C_f)$ is calculated by adding the individual systematic uncertainties in quadrature and is found to be 0.012 (0.016). The main sources of systematic uncertainty are listed in Tables III and IV.

For the $\eta_c K_S^0$ mode, we found $-\eta_f S_f = 0.925 \pm 0.160(\text{stat}) \pm 0.057(\text{syst})$, which has a significance of 5.4σ standard deviations including systematic uncertainties. Our result is the first observation of CP violation in this mode.

VIII. CONCLUSIONS

We report improved measurements of the time-dependent CP asymmetry parameters. The results in this paper supercede those of our previous publication [5]. We report our measurements in terms of C_f and S_f. We find

$$C_f = 0.024 \pm 0.020(\text{stat}) \pm 0.016(\text{syst}),$$
$$-\eta_f S_f = 0.687 \pm 0.028(\text{stat}) \pm 0.012(\text{syst}),$$

providing an independent constraint on the position of the apex of the unitarity triangle [17]. Our measurements agree

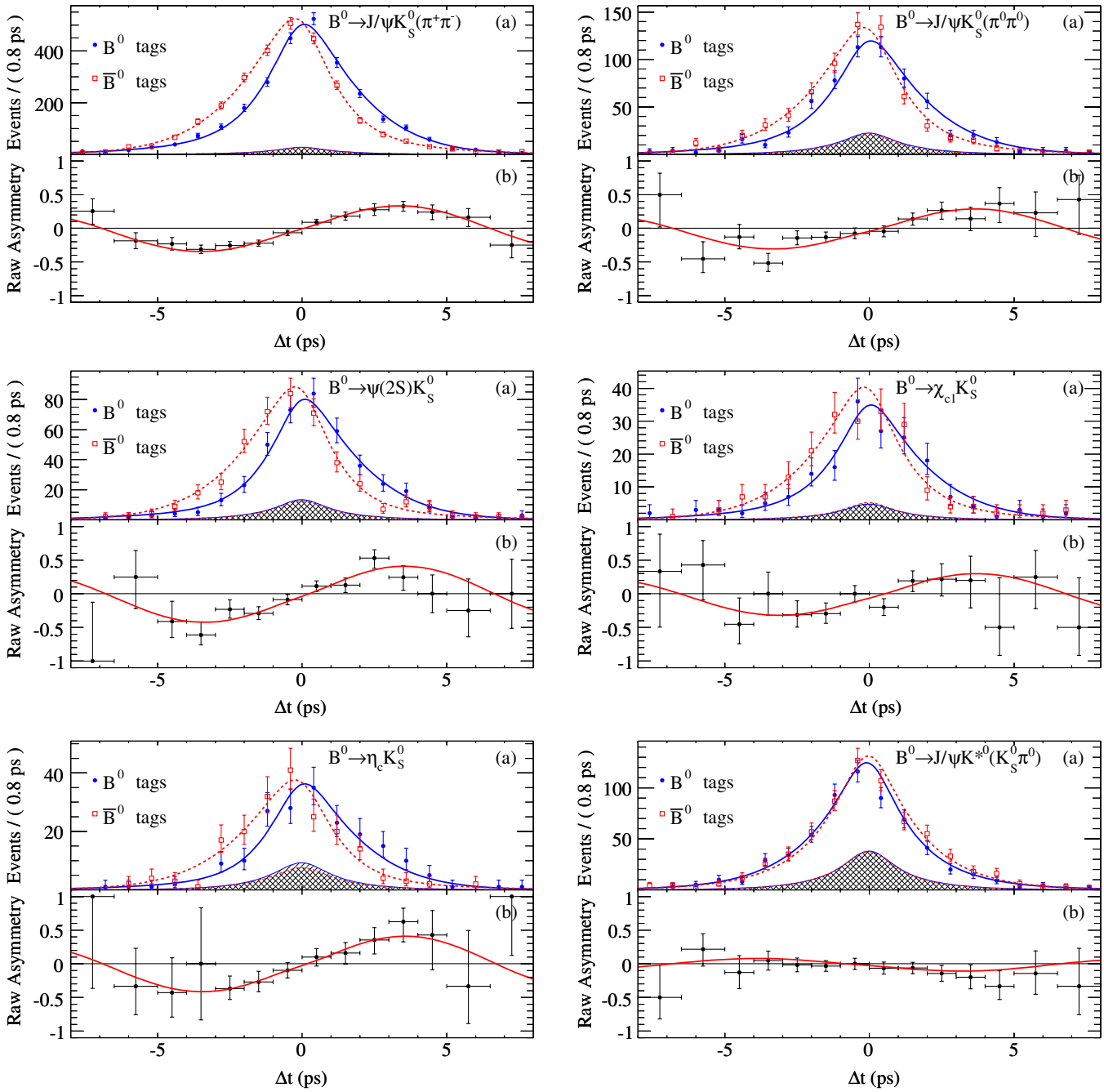

FIG. 4 (color online). (a) Number of B^0 candidates in the signal region with a B^0 tag (N_{B^0}) and with a $\bar{B}^0$ tag ($N_{\bar{B}^0}$), and (b) the corresponding raw asymmetry, $(N_{B^0} - N_{\bar{B}^0})/(N_{B^0} + N_{\bar{B}^0})$, as functions of Δt for each B^0 decay mode. The solid (dashed) curves represent the fit projections in Δt for $B^0(\bar{B}^0)$ tags. The right-hatched (left-hatched) shaded regions represent the estimated background contributions in $\bar{B}^0(B^0)$ tagged events.

with previous published results [5,18] and with the theoretical estimates of the magnitudes of CKM matrix elements within the context of the SM [19]. We also report measurements of C_f and S_f for each decay mode in our *CP* sample and for the combined $J/\psi K^0(K_S^0 + K_L^0)$ mode. *CP* violation in $\eta_c K_S^0$ mode is established at the level of 5.4σ standard deviations including systematic uncertainties.

ACKNOWLEDGMENTS

We are grateful for the extraordinary contributions of our PEP-II colleagues in achieving the excellent luminosity and machine conditions that have made this work possible. The success of this project also relies critically on the expertise and dedication of the computing organizations that support *BABAR*. The collaborating institutions

TABLE III. Main systematic uncertainties on S_f and C_f for the full CP sample, and for the $J/\psi K^0$, $J/\psi K_S^0$, and $J/\psi K_L^0$ samples. For each source of systematic uncertainty, the first line gives the error on S_f and the second line the error on C_f. The total systematic error (last row) also includes smaller effects not explicitly mentioned in the table.

Source/sample		Full	$J/\psi K^0$	$J/\psi K_S^0$	$J/\psi K_L^0$
Beam spot	S_f	0.001	0.002	0.003	0.000
	C_f	0.001	0.001	0.002	0.000
Mistag differences	S_f	0.006	0.006	0.006	0.006
	C_f	0.002	0.002	0.002	0.002
Δt resolution	S_f	0.007	0.007	0.007	0.007
	C_f	0.003	0.003	0.003	0.007
$J/\psi K_L^0$ background	S_f	0.006	0.006	0.000	0.027
	C_f	0.001	0.001	0.000	0.004
Background fraction and CP content	S_f	0.005	0.004	0.004	0.004
	C_f	0.003	0.002	0.001	0.011
$m_{\rm ES}$ parametrization	S_f	0.002	0.002	0.003	0.001
	C_f	0.000	0.001	0.001	0.000
Δm_d, τ_B, $\Delta\Gamma_d/\Gamma_d$	S_f	0.003	0.003	0.004	0.004
	C_f	0.001	0.001	0.001	0.001
Tag-side interference	S_f	0.001	0.001	0.001	0.001
	C_f	0.014	0.014	0.014	0.014
Fit bias (MC statistics)	S_f	0.002	0.004	0.004	0.006
	C_f	0.003	0.004	0.004	0.006
Total	S_f	0.012	0.013	0.012	0.031
	C_f	0.016	0.018	0.016	0.027

wish to thank SLAC for its support and the kind hospitality extended to them. This work is supported by the U.S. Department of Energy and National Science Foundation, the Natural Sciences and Engineering Research Council (Canada), the Commissariat à l'Energie Atomique and Institut National de Physique Nucléaire et de Physique des Particules (France), the Bundesministerium für Bildung und Forschung and Deutsche Forschungs-

TABLE IV. Main systematic uncertainties on S_f and C_f for the $J/\psi K_S^0(\pi^+\pi^-)$, $J/\psi K_S^0(\pi^0\pi^0)$, $\psi(2S)K_S^0$, $\chi_{c1}K_S^0$, $\eta_c K_S^0$, and $J/\psi K^{*0}(K^{*0}\to K_S^0\pi^0)$ decay modes. For each source of systematic uncertainty, the first line gives the error on S_f and the second line the error on C_f. The total systematic error (last row) also includes smaller effects not explicitly mentioned in the table.

Source/sample		$J/\psi K_S^0(\pi^+\pi^-)$	$J/\psi K_S^0(\pi^0\pi^0)$	$\psi(2S)K_S^0$	$\chi_{c1}K_S^0$	$\eta_c K_S^0$	$J/\psi K^{*0}$
Beam spot	S_f	0.003	0.002	0.008	0.028	0.001	0.006
	C_f	0.002	0.003	0.009	0.012	0.000	0.000
Mistag differences	S_f	0.006	0.006	0.006	0.006	0.006	0.006
	C_f	0.002	0.002	0.002	0.002	0.002	0.002
Δt resolution	S_f	0.007	0.007	0.007	0.010	0.016	0.026
	C_f	0.003	0.004	0.007	0.004	0.004	0.006
$J/\psi K_L^0$ background	S_f	0.000	0.000	0.000	0.000	0.000	0.000
	C_f	0.000	0.000	0.000	0.000	0.000	0.000
Background fraction and CP content	S_f	0.003	0.007	0.016	0.017	0.051	0.056
	C_f	0.001	0.003	0.006	0.010	0.019	0.026
$m_{\rm ES}$ parametrization	S_f	0.002	0.009	0.024	0.006	0.002	0.037
	C_f	0.001	0.006	0.001	0.002	0.001	0.008
Δm_d, τ_B, $\Delta\Gamma_d/\Gamma_d$	S_f	0.003	0.007	0.016	0.003	0.016	0.014
	C_f	0.001	0.001	0.001	0.001	0.002	0.001
Tag-side interference	S_f	0.001	0.001	0.001	0.001	0.001	0.001
	C_f	0.014	0.014	0.014	0.014	0.014	0.014
Fit bias (MC statistics)	S_f	0.005	0.004	0.008	0.007	0.007	0.027
	C_f	0.004	0.003	0.002	0.004	0.007	0.039
Total	S_f	0.012	0.017	0.036	0.040	0.057	0.087
	C_f	0.016	0.018	0.020	0.025	0.029	0.054

gemeinschaft (Germany), the Istituto Nazionale di Fisica Nucleare (Italy), the Foundation for Fundamental Research on Matter (The Netherlands), the Research Council of Norway, the Ministry of Education and Science of the Russian Federation, Ministerio de Educación y Ciencia (Spain), and the Science and Technology Facilities Council (United Kingdom). Individuals have received support from the Marie-Curie IEF program (European Union) and the A. P. Sloan Foundation.

[1] N. Cabibbo, Phys. Rev. Lett. **10**, 531 (1963); M. Kobayashi and T. Maskawa, Prog. Theor. Phys. **49**, 652 (1973).
[2] A. B. Carter and A. I. Sanda, Phys. Rev. D **23**, 1567 (1981); I. I. Bigi and A. I. Sanda, Nucl. Phys. **B193**, 85 (1981).
[3] W.-M. Yao *et al.* (Particle Data Group), J. Phys. G **33**, 1 (2006).
[4] See, for example, D. Kirkby and Y. Nir, p. 146 in Ref. [3].
[5] B. Aubert *et al.* (*BABAR* Collaboration), Phys. Rev. Lett. **99**, 171803 (2007).
[6] Charge conjugation is implied throughout this paper.
[7] B. Aubert *et al.* (*BABAR* Collaboration), Phys. Rev. D **76**, 031102(R) (2007).
[8] PEP-II Conceptual Design Report, SLAC Report No. SLAC-R-418, 1993.
[9] B. Aubert *et al.* (*BABAR* Collaboration), Nucl. Instrum. Methods Phys. Res., Sect. A **479**, 1 (2002).
[10] W. Menges, IEEE Nucl. Sci. Symp. Conf. Rec. **5**, 1470 (2006).
[11] S. Agostinelli *et al.* (GEANT4 Collaboration), Nucl. Instrum. Methods Phys. Res., Sect. A **506**, 250 (2003).
[12] D. Lange, Nucl. Instrum. Methods Phys. Res., Sect. A **462**, 152 (2001).
[13] B. Aubert *et al.* (*BABAR* Collaboration), Phys. Rev. D **66**, 032003 (2002).
[14] H. Albrecht *et al.* (ARGUS Collaboration), Phys. Lett. B **241**, 278 (1990).
[15] O. Long, M. Baak, R. N. Cahn, and D. Kirkby, Phys. Rev. D **68**, 034010 (2003).
[16] B. Aubert *et al.* (*BABAR* Collaboration), Phys. Rev. D **73**, 111101 (2006).
[17] See, for example, A. Ceccucci, Z. Ligetti, and Y. Sakai, p. 138 in Ref. [3].
[18] K. F. Chen *et al.* (Belle Collaboration), Phys. Rev. Lett. **98**, 031802 (2007).
[19] M. Ciuchini *et al.*, Z. Phys. C **68**, 239 (1995).